

Superconducting Niobium RF Cavities Designed to Attain High Surface Electric Fields

D.L. Moffat, T. Flynn, J. Kirchgessner, H. Padamsee, D. Rubin, J. Sears, Q. Shu*
Laboratory of Nuclear Studies, Cornell University, Ithaca, NY 14853-5001

Abstract

Two cavities have been designed to study the behavior of superconducting niobium cavities at high surface electric fields. The first, designated Mark I, is a completely welded cavity which has been tested several times. After some initial difficulties with low Q_0 values we were able to reach a Q_0 of $\sim 3 \times 10^9$ at 1.5K at low fields. Upon raising the RF power we encountered several multipacting barriers that successfully processed away. Ultimately we were able to apply all of the available RF power (20 watts) to reach a surface electric field of 145 MV/m and a corresponding magnetic field of 1345 gauss. Emission was observed but we are uncertain of its source. The second cavity, designated Mark II, has been designed with a removable baseplate which is attached to the cavity with an indium seal. This cavity has achieved a Q_0 of $\sim 9 \times 10^9$ at 1.5K at low fields. The multipacting barriers in this cavity occur at relatively low fields, ~ 10 MV/m peak surface electric field, and do not yield to processing. Ultimately thermal breakdown occurs. The cause of this strong multipacting is under investigation.

* Work supported by the National Science Foundation with supplemental funding from the US-Japan agreement

Introduction

Among the most basic questions pertaining to the high field capability of superconducting niobium cavities is whether the niobium surface, under any condition, will tolerate the surface electric fields required for its incorporation into a particle accelerator. DC fields as high as 200 MV/m have been achieved over surfaces as large as a square centimeter [1]. The highest RF surface field ever achieved, however, had been only 70 MV/m [2]. The typical niobium accelerating cavity design requires that a cavity operating near the theoretical magnetic field limit of 2000 gauss be capable of supporting a surface electric field of ~ 100 MV/m.

Heat treated 1500 MHz single cell accelerating cavities in our laboratory now frequently reach peak surface fields of 40 - 53 MV/m (the peak field occurs where the beam tubes join the cavity, i.e. the irises) [3]. Evidence to date suggests that under many circumstances emitters are extrinsic to the niobium walls of the cavity. The probability of encountering such emitters in a certain region of a cavity is proportional to the surface area of that region. The irises of an accelerating cavity constitute a relatively large area and, therefore, there is a high probability that an emitter will be found there. Because this is the region of the highest electric fields, an emitter here will limit the application of higher fields elsewhere. Thus, by limiting the area of the high field region of a cavity we may be able to determine the intrinsic capabilities of niobium. Conversely, we may be able to create or place an emitter in a controlled manner at a position where it will dominate the performance of the cavity. In this way more information about the nature of actual emitters may be obtained and effective processing techniques developed.

These ideas have led us to develop two new cavities. A standard niobium S-band accelerating cavity half-cell is closed off near the equator with a niobium plate. In the Mark I cavity this plate is welded to the half-cell. The baseplate in the Mark II cavity is attached with an indium O-ring. The modes studied are non-accelerating higher order monopole modes in which the area exposed to the highest electric fields is very small. In addition, the fields in this region are 4-6 times higher than anywhere else in the cavity, depending on the mode. The ratio of peak surface magnetic field to peak surface electric field is also quite favorable, e.g. at 100 MV/m the peak surface magnetic field is 1000-1200 gauss.

The Mark I Design

Calculations and Copper Model Tests

The Mark I cavity design is shown in Figure 1. It was designed around existing S-band niobium half-cells. The frequency of the TM_{010} mode in an accelerating cavity using these cells is about 2856 MHz. It was known that placing a metallic plate at the equator of an accelerating cavity would create high E fields on the plate in a mode at roughly twice the frequency of the fundamental [4]. Since any protrusion into the fields would enhance the fields there, it was decided to put a dimple at the center of the baseplate. The dimensions of the dimple were determined by deep drawing considerations. The radius of curvature on the perimeter of the baseplate was set at .25", also for ease of deep drawing. Armed with this information we used URMEL and URMELT to calculate the mode spectrum of such a cavity to identify suitable modes (the side port had to be omitted for these calculations) [5]. The beam tube was designed to be a cutoff tube at 2856 GHz but it was clear that it would not be cutoff at 6 GHz. In fact, the URMEL/T calculations demonstrated that the beam tube was an integral part of the cavity and helped to create the desired field pattern at the dimple. If the beam tube diameter was reduced to create a cutoff tube, the field pattern was not completely suitable.

Table 1 shows the results of URMEL and SUPERFISH calculations of the monopole modes of this cavity [6]. These codes indicate that the field enhancement at the dimple is greatest in the TM_{011} mode, but quite attractive in the TM_{020} mode as well. (These mode classifications pertain to the Mark I cavity and not to the accelerating cavity upon which it is based. The same modes may be classified differently in an accelerating cavity.) The mode at 6987 MHz is a resonance of the beam tube. The electric field patterns for the TM_{020} and TM_{011} modes, as calculated by URMEL, are shown in Figure 2. Figure 3 shows the results of SUPERFISH calculations for the surface electric field as a function of position along the niobium surface for both modes. The fields have been normalized to 100 MV/m at the dimple to facilitate comparison. For the TM_{020} mode, the E field at the dimple is 4.4 times the next highest field, which occurs on the baseplate, but not in the vicinity of the dimple. The enhancement factor is 6.5 for the TM_{011} mode, with the next highest field occurring at what would be the iris in an accelerating cavity. For comparison, in the same cavity, but without the dimple, the enhancement at the center of the baseplate is only 1.8 in the TM_{020} mode, 3.6 in the TM_{011} mode.

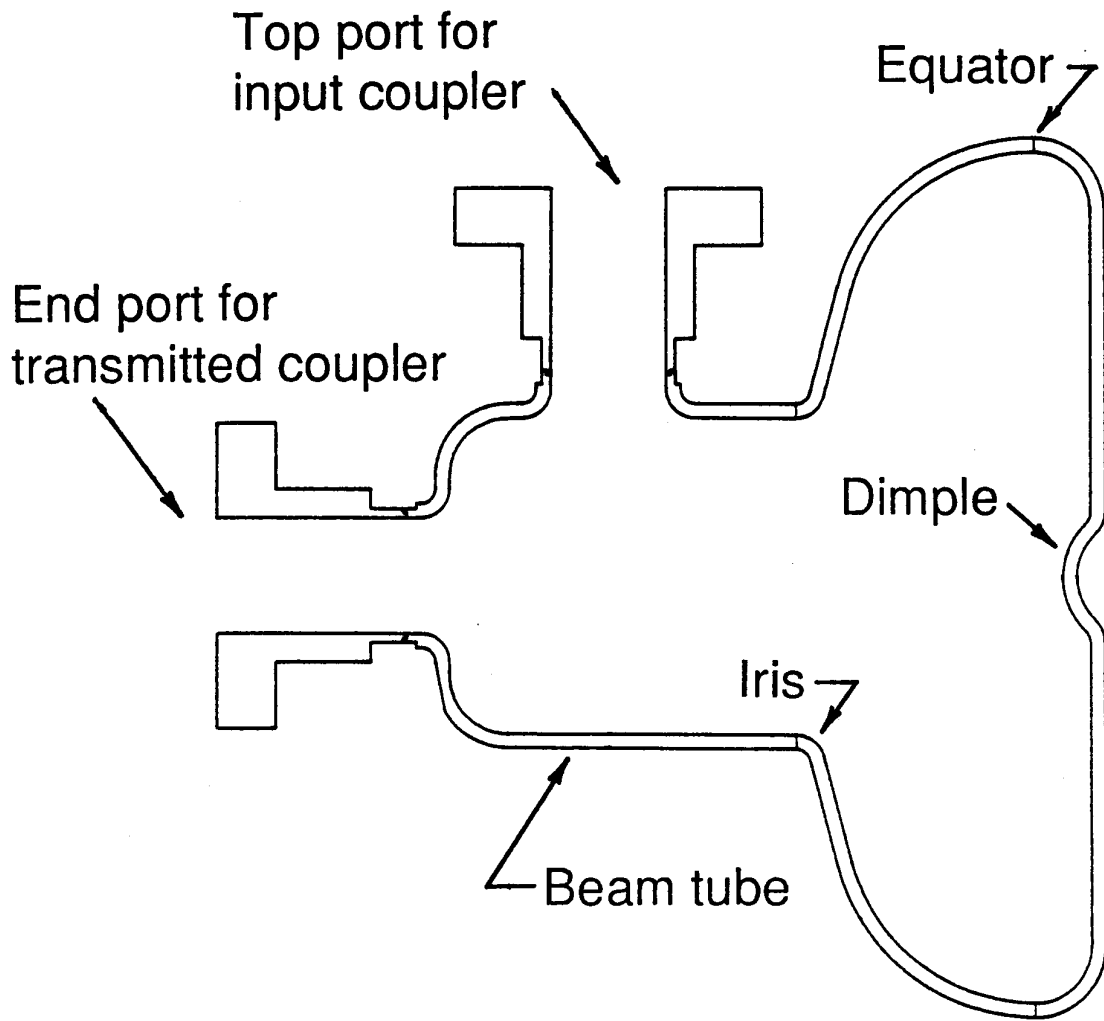


FIGURE 1 The Mark I cavity design

TABLE 1

Mark I Monopole Modes

URMEL calculations					
<u>Mode</u>	<u>MHz</u>	<u>Q_{Cu}</u>	<u>E_{pk}/√U</u>	<u>H_{pk}/E_{pk}</u>	<u>E_{pk}/E_{next}</u>
TM ₀₁₀	2736.89	13620	147.1	9.6	2.2
TM ₀₂₀	5772.59	19763	186.0	9.3	4.4
TM ₀₁₁	6592.21	16694	232.8	11.2	6.5
Tube	6986.61	17780			
			MV/m/√J	G/MV/m	
SUPERFISH calculations					
<u>Mode</u>	<u>MHz</u>	<u>Q_{Cu}</u>	<u>E_{pk}/√U</u>	<u>H_{pk}/E_{pk}</u>	<u>E_{pk}/E_{next}</u>
TM ₀₁₀	2739.24	14328	145.5	9.0	2.2
TM ₀₂₀	5778.50	20921	185.0	8.8	4.0
TM ₀₁₁	6597.76	17365	229.4	12.1	7.0
			MV/m/√J	G/MV/m	

TABLE 2

Mark I Mode Spectrum

<u>Mode type</u>	<u>MHz</u>	<u>Q_{Cu}</u>	<u>G (Ω)</u>	<u>Q_{4.2}</u>	<u>Q_{1.5}</u>
TM ₀₁₀	2736.89	13620	176.4	5.79x10 ⁷	5.00x10 ¹⁰
Dipole	3981.03	16306	268.5	4.65	4.14
Dipole	4992.83	16408	302.6	3.57	3.25
Quadrupole	5362.47	18809	359.5	3.77	3.45
TM ₀₂₀	5772.59	19763	417.6	3.84	3.55
Dipole	6076.17	17110	348.1	2.96	2.75
Quadrupole	6479.37	19877	417.6	3.19	2.99
TM ₀₁₁	6592.21	16694	364.8	2.71	2.54
Sextupole	6632.60	20812	442.4	3.26	3.06
TE ₀₁₁	6704.39	16033			
Dipole	6909.74	18911	410.3	2.82	2.66
Tube	6986.61	17780	403.0	2.68	2.53

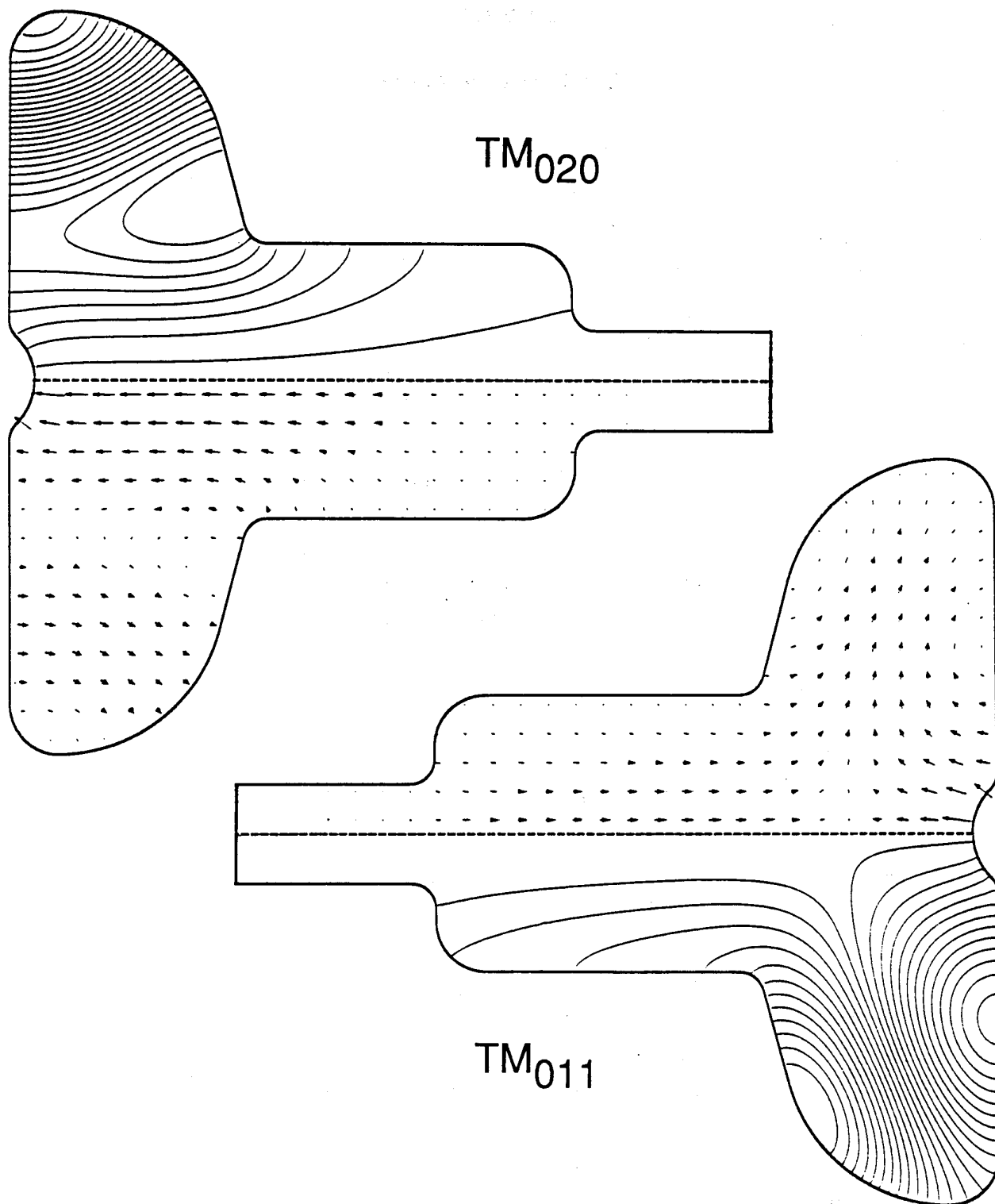


FIGURE 2 Electric field patterns of the TM_{020} and TM_{011} modes in the Mark I cavity

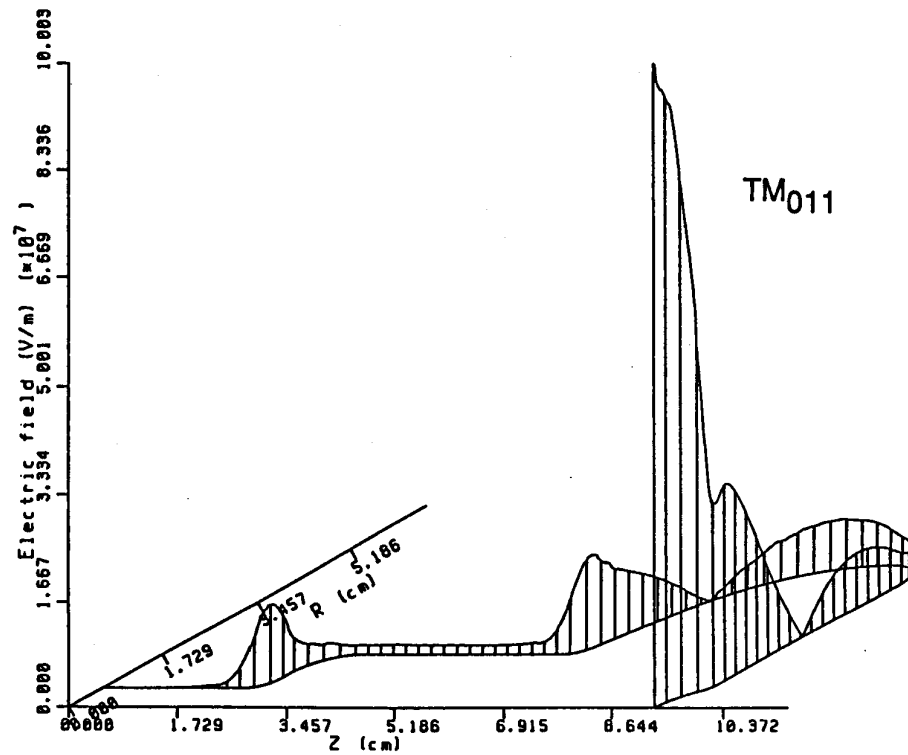
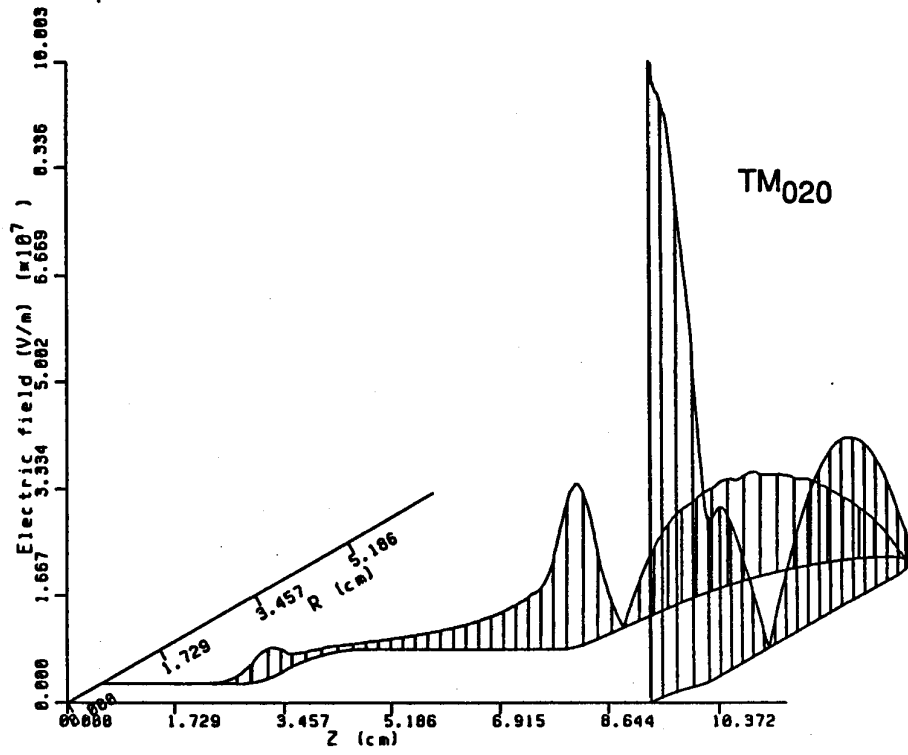


FIGURE 3 Surface electric fields of the TM_{020} and TM_{011} modes in the Mark I cavity

It was noted earlier that the probability of an emitter occurring in a given field region of a cavity was proportional to the surface area of that region. Figure 4 shows plots of surface area exposed to a given electric field when the peak surface electric field is 100 MV/m for the TM_{020} and TM_{011} modes. The total area exposed to fields within 50% of the maximum is only 79 mm² in the TM_{020} mode, 101 mm² in the TM_{011} mode. This is in contrast to 10100 mm² under the same conditions in a 1500 MHz accelerating cavity.

There are a great many other modes in this cavity beside the interesting monopoles. Table 2 gives the complete mode spectrum up to 7 GHz. The geometry factor, G, is the product of R, the RF surface resistance of the cavity walls, and the cavity Q_0 . The Q_0 values given for 4.2 and 1.5K assume the BCS resistance of niobium calculated using the program of Halbritter [7]. Since actual cavities are always somewhat asymmetric, it can be expected that all of the dipole, quadrupole and sextupole modes will each be slightly polarized, and thus be split in frequency. This will result in 12 modes between 5773 and 6987 MHz. The number of modes in the vicinity of the TM_{011} mode could make it difficult to identify during a test. On the other hand, the TM_{020} mode is relatively free of neighbors.

Bench measurements were made on a copper model of the Mark I cavity. Power was coupled into the cavity using an antenna in the top port. Because the coupling from the end port was too weak for accurate measurements, the transmitted coupler was placed on the base plate of the cavity, approximately halfway between the dimple and the equator. Even here, 60 dB amplification of the transmitted signal was required. In order to identify the modes which have two polarizations, holes were drilled at 45° intervals around the equator and a 1/16" sapphire rod inserted across the diameter of the cavity. The sapphire rod cleared the dimple by about 3/16". Along the diameter, the sapphire rod affected the splitting of the dipole, quadrupole and sextupole modes and had little effect on the monopole modes. On axis, however, the sapphire rod greatly affected the frequencies of the monopole modes.

When the niobium cavity is tested in liquid helium it is under vacuum. This raises the additional problem of baseplate deflection due to evacuation of the cavity. This was simulated in the copper cavity by deflecting the baseplate with a C-clamp. The copper cavity measurements are shown in Figure 5. The TM_{020} mode is relatively unaffected by baseplate deflection. However, baseplate deflection results in the sextupole and TM_{011} modes crossing each other at about .020" of deflection. This greatly complicates the identification of the different modes. URMEL was run for the monopole and sextupole modes and verified the experimental results. As the deflection increases, the TM_{020} mode

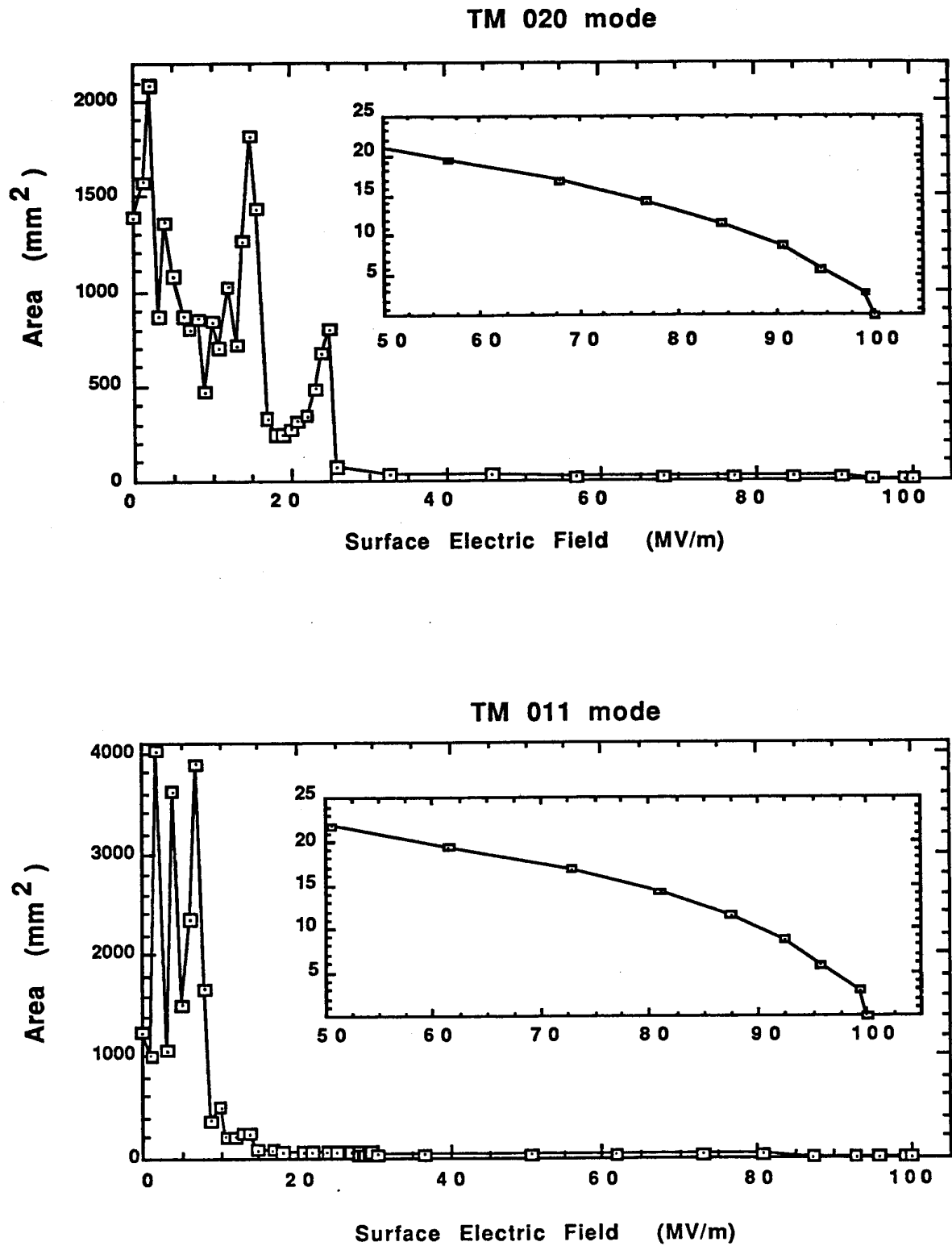


FIGURE 4 Cavity surface area exposed to a given electric field in the Mark I cavity

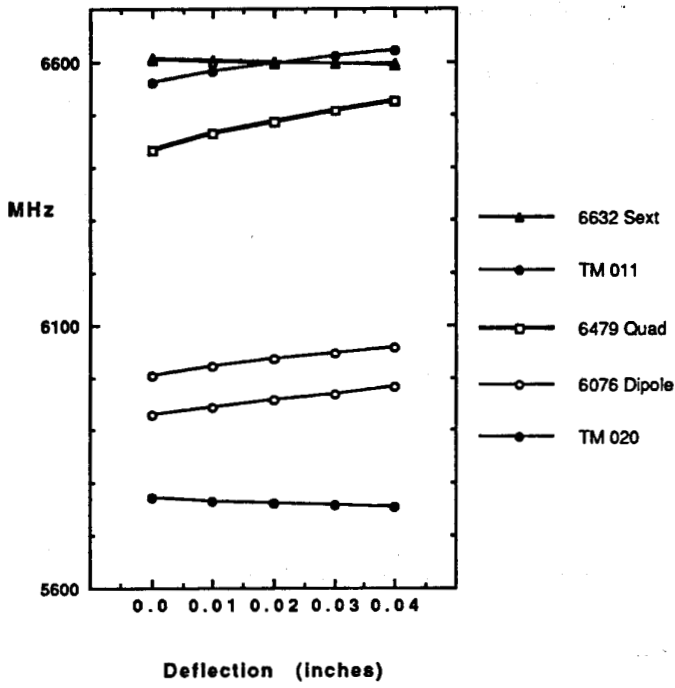


FIGURE 5 The effect of baseplate deflection on frequency in a copper model of the Mark I cavity

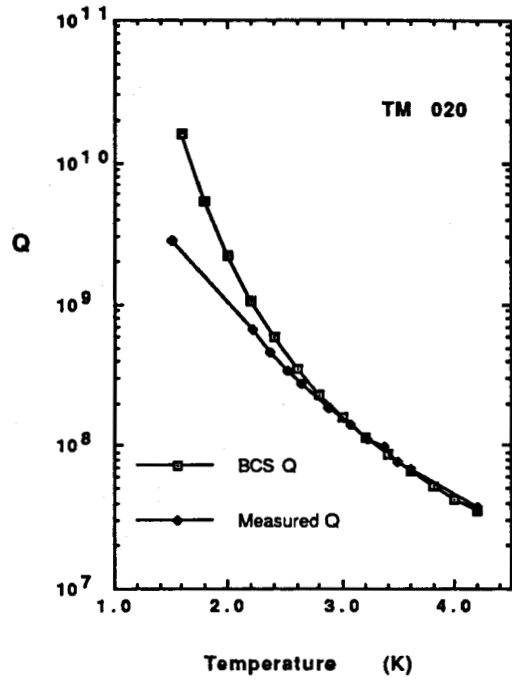


FIGURE 6 Q_0 as a function of temperature in the Mark I cavity

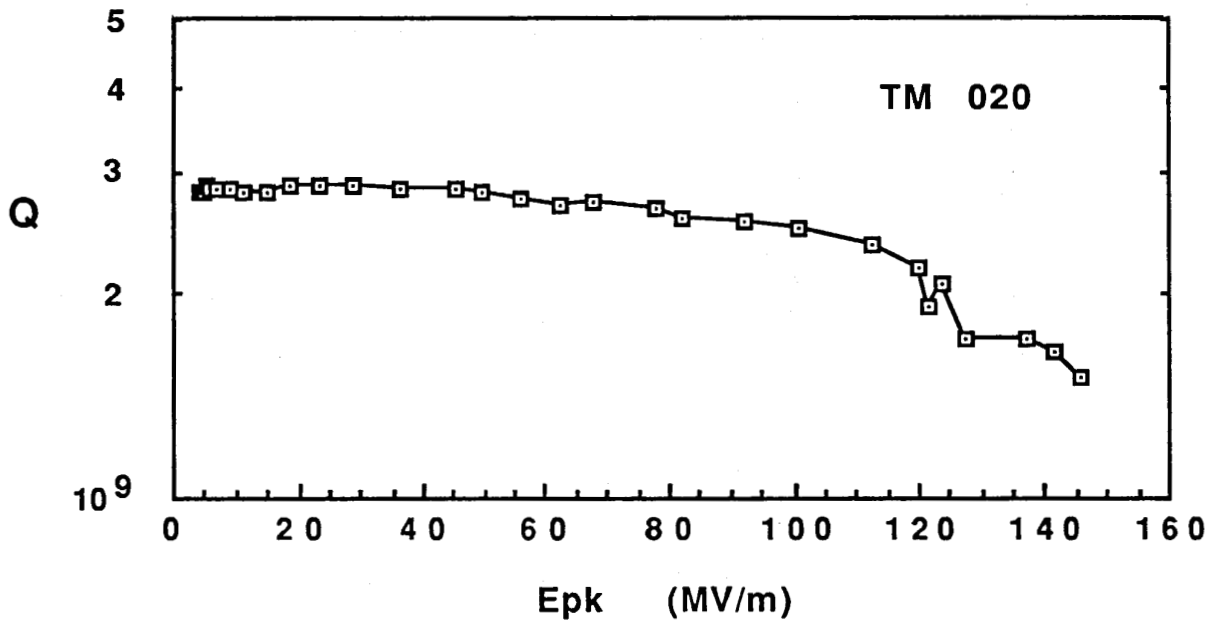


FIGURE 7 Q_0 as a function of peak surface field in the Mark I cavity at ~1.5K

continues to drop in frequency and remains clear of the other modes. The frequency of the TM_{011} mode, as well as that of the neighboring quadrupole mode, increases and eventually converges on that of the dipole mode at 6910 MHz. At such severe deflections, e.g. around .16", it becomes extremely difficult to identify the TM_{011} mode. Table 3 summarizes the important results for the TM_{020} and TM_{011} modes. These data indicate that the degree of deflection should be known in order to accurately calculate the electric field at the dimple.

TABLE 3

Bowed Baseplate Calculations

<u>Deflection</u>	TM_{020}		TM_{011}	
	<u>MHz</u>	<u>E_{pk}/\sqrt{U}</u>	<u>MHz</u>	<u>E_{pk}/\sqrt{U}</u>
.000"	5772.59	186.0	6592.21	232.8
.030	5757.80	188.0	6639.77	226.6
.080	5733.06	191.9	6720.85	216.3
.156	5690.85	217.1	6838.90	212.4
		MV/m/ \sqrt{J}		MV/m/ \sqrt{J}

Niobium Cavity Tests

Two Mark I cavities were made using 1/16" thick niobium with a RRR of ~250. All pieces were joined with electron beam welds. The cavity was attached to the test stand using an indium O-ring on the top port, resulting in the baseplate of the cavity being mounted vertically during testing. The input coupler was an antenna which was inserted into the top port. This arrangement prevented debris from the sliding contact on the outer conductor of the coupler from falling directly on the high field dimple. When used, a transmitted coupler was placed on the end port. After initial evacuation with a separate turbo pump, an ion pump maintained the vacuum at $<10^{-7}$ torr.

In several early tests we encountered difficulties in obtaining Q_0 values over $\sim 5 \times 10^8$ at 1.5K. This limited the surface electric fields to ~ 34 MV/m for our maximum input power of 20 W. In these tests we used the standard chemical etching surface treatment that is applied to accelerating cavities. Suspecting that acid treatment of a closed cavity was part

of our problem, we heat-treated one cavity for 2.5 hours at 900°C in our UHV furnace. This choice of temperature was guided by the desire to drive out any hydrogen which may have been dissolved in the bulk, while at the same time preserving the high initial RRR. One side-effect of this heat-treatment was to anneal the cavity, allowing the baseplate to deflect .156" from the nominal flat position when it was evacuated. With this severe deformation it was impossible to identify the TM_{011} mode, though the TM_{020} mode could be studied easily.

Subsequently, we discovered and eliminated debris from the test stand and RF feedline which was another source of our low Q_0 problems. The cavity was ultrasonically cleaned upside-down for 2 hours in methanol after which the cavity obtained a Q_0 of 3.7×10^7 at 4.2K at 5683 MHz (TM_{020}). This value was in agreement with the BCS Q. Figure 6 shows that during cooldown the cavity Q_0 continued to remain at the BCS level until about 2K. The residual Q_0 was $\sim 2.8 \times 10^9$. The BCS Q at 1.5K is $\sim 3.6 \times 10^{10}$.

Q_0 vs peak surface electric field for the best test is shown in Figure 7. The downward curvature of this graph above 100 MV/m is characteristic of field emission. In our 1500 MHz accelerating cavities Q_0 can drop by more than an order of magnitude due to FE loading. This suggests that FE loading had not yet become severe. The cavity was finally able to reach a peak surface electric field of 145 MV/m at the dimple. The corresponding surface magnetic field was 1345 gauss.

There were several multipacting barriers which were processed quickly on the way to 145 MV/m. Multipacting began at a peak field of ~ 45 MV/m and continued up to ~ 100 MV/m at which point x-rays were first detected at the top of the dewar. The power was raised until the x-ray intensity exceeded the limits for safe operation with the existing shielding. Because the shielding could not be increased during this test, no helium processing was attempted to increase either Q_0 or E_{pk} . In addition, our high power capability at 6000 MHz is only 20 W and we were very close to that limit as well.

A plot of P_{diss} vs E_{pk}^2 shows a deviation from linearity at about 77 MV/m. The data are shown in Figure 8. When the difference in measured and calculated P_{diss} is plotted vs $1/E_{pk}$, the typical Fowler-Nordheim plot is obtained (Figure 9). Since the location of the emitter is unknown the actual field at the emitter is also unknown, precluding an accurate calculation of the β , the Fowler-Nordheim enhancement factor, of the emitter.

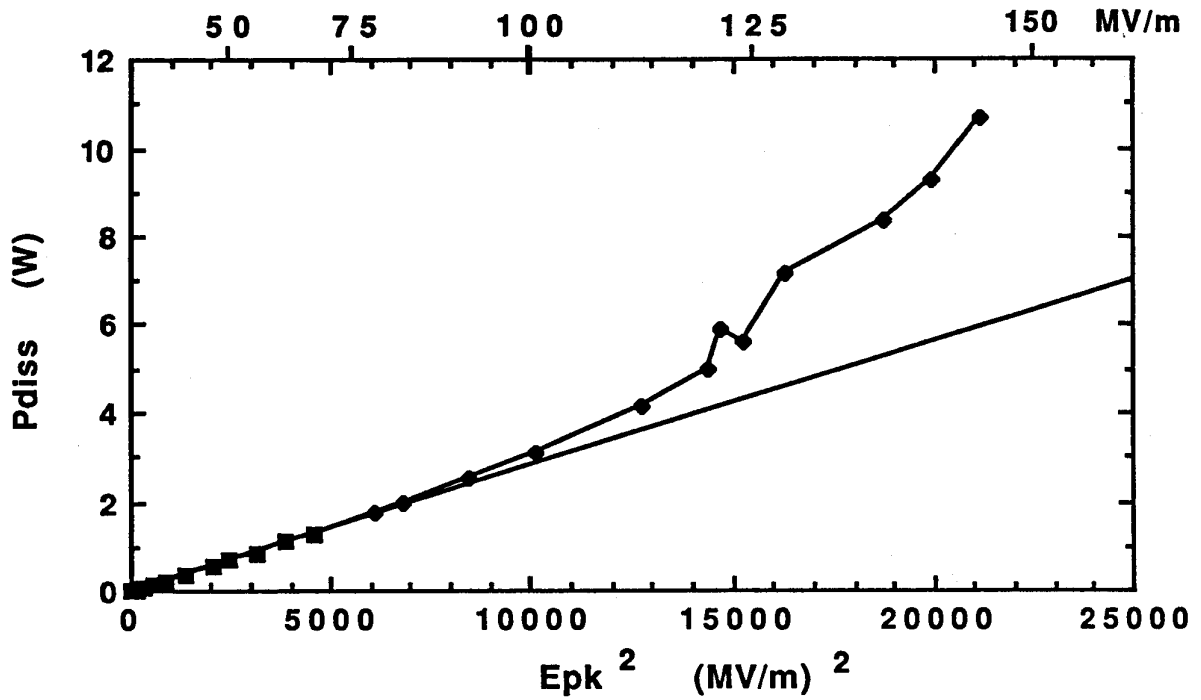


FIGURE 8 Dissipated power in the Mark I cavity at ~ 1.5 K

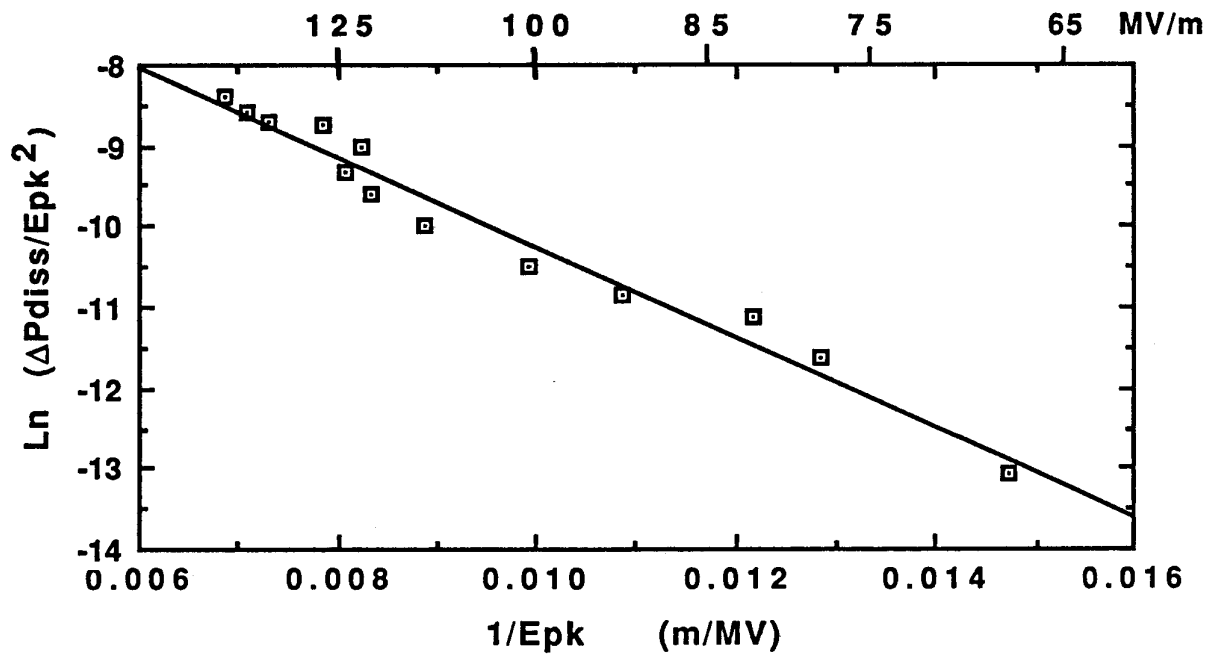


FIGURE 9 Fowler-Nordheim plot from the Mark I cavity at ~ 1.5 K

In a subsequent test of the same cavity we achieved ~ 80 MV/m with a Q_0 of 1.7×10^9 . The peak magnetic surface field was ~ 740 gauss. In this test we were limited by thermal breakdown.

The Mark II Design

Calculations and Copper Model Tests

The Mark II cavity is shown in Figure 10. The coupling ports, beam tube and half-cell are identical to that of the Mark I design. The design of this cavity was driven by the desire to be able to remove the high field region of the cavity and examine it in a scanning electron microscope without introducing artifacts during removal which could be misconstrued as being emission sites. An equally important criterion was to avoid a design which would result in a low cavity Q_0 because of the currents which would inevitably cross the indium joint. Several schemes were evaluated after which it was decided to make the entire baseplate removable.

During the design process it was noticed that the TM_{011} mode had a magnetic field null on the wall of the half-cell (no current crosses this null, thus it is an ideal location for an indium joint). By extending the wall of the half-cell, the cavity was lengthened, lowering the frequency of the TM_{011} mode and drawing the field null into the corner of the cavity. In a perfectly machined cavity this would be sufficient to produce high Q_0 's. The additional length required to position the current null in the cavity corner was determined by URMEL to be .375". A copper model without the choke joint was made to verify these calculations. The Q of the copper cavity was measured as a function of side-wall extension. To make these measurements more sensitive, a carbon conducting paper or acetate film gasket was inserted in the joint. Figure 11 shows that when the current null is in the corner, the Q is unaffected by the resistance of the joint.

Past experience with TE_{011} cavities has shown that it is extremely difficult to fabricate a niobium cavity with an indium joint at a theoretical current null and attain Q_0 values greater than 10^9 . For this reason a choke joint was designed for the Mark II cavity in the TM_{011} mode. This joint yields a virtual short at the corner of the cavity by producing a real short a distance of $\sim \lambda/2$ away. At roughly $\lambda/4$ from these two points is a current null at which the indium joint can be placed. The amount of field in the choke groove is determined by the

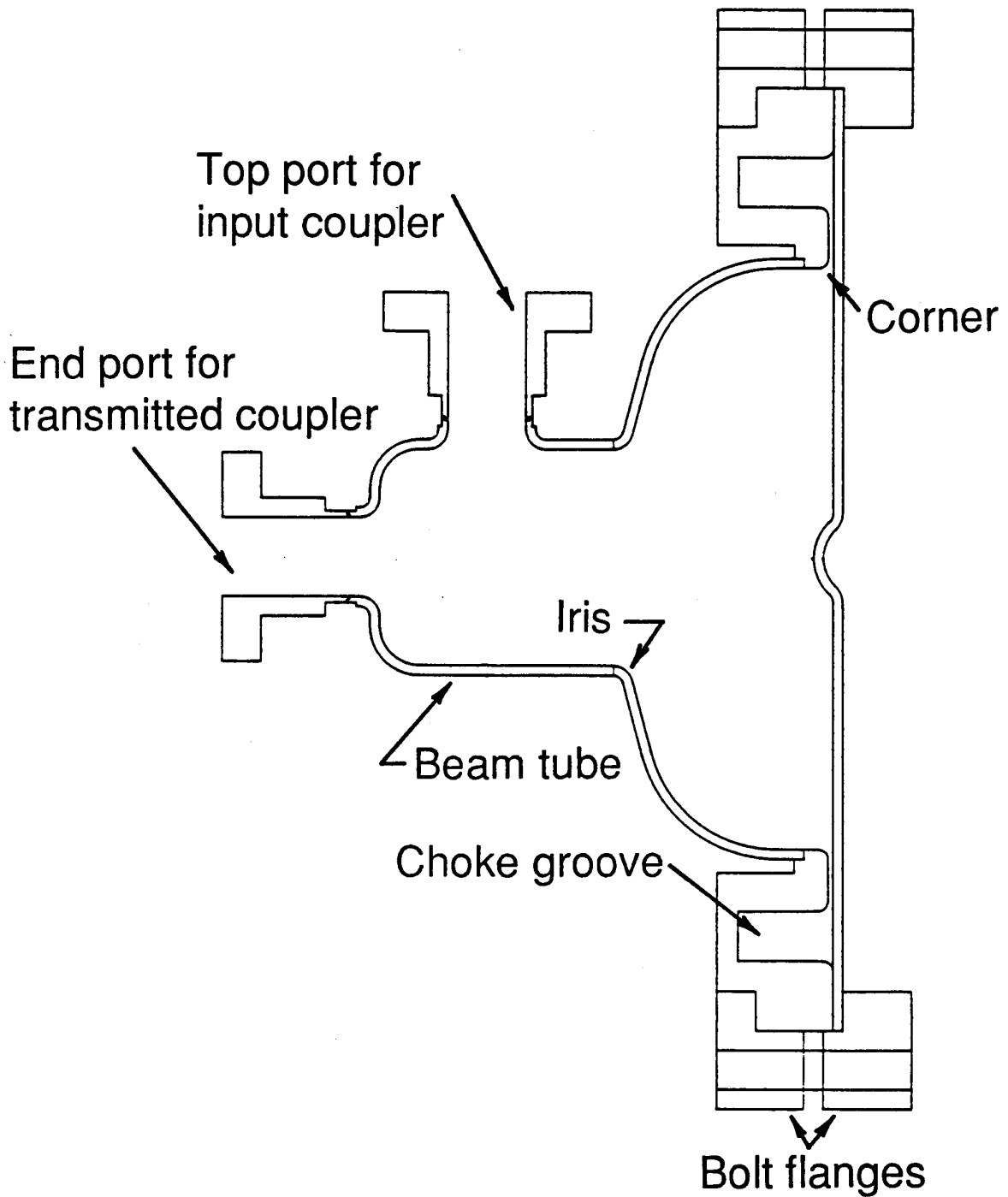


FIGURE 10 The Mark II cavity design. The baseplate is joined to the cavity using an indium O-ring.

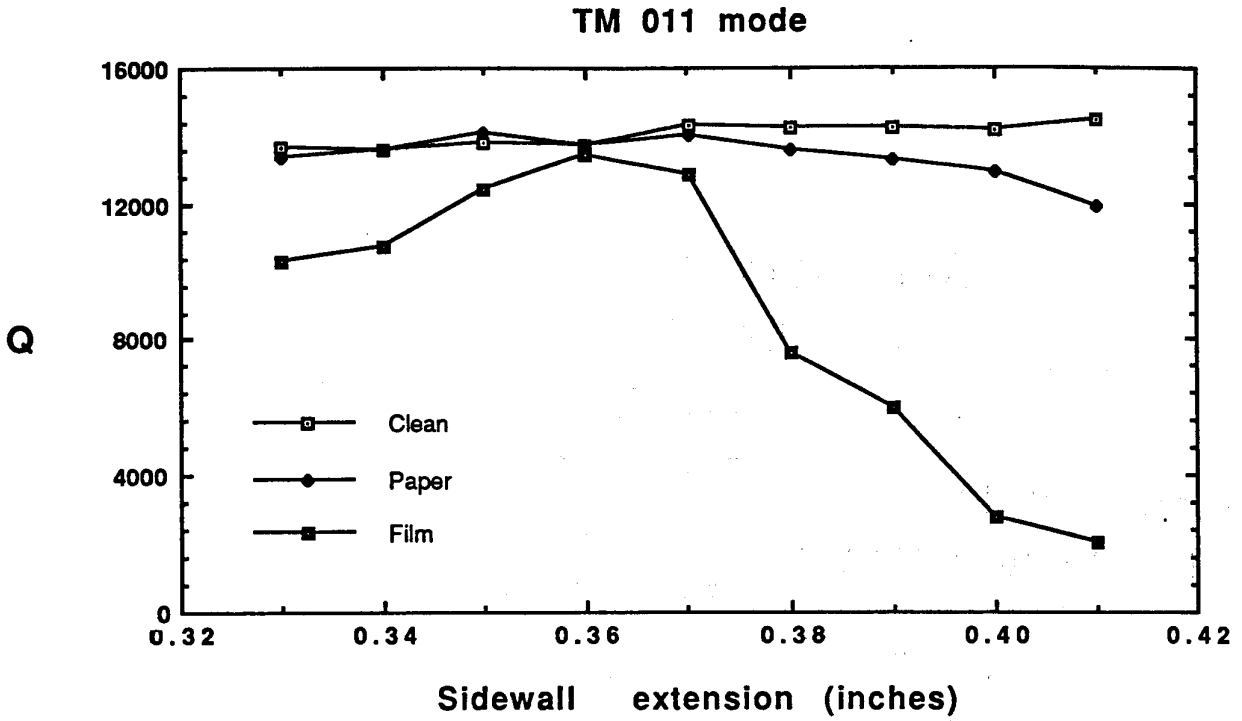


FIGURE 11 Q as a function of extension in a copper model of the Mark II cavity. There was no choke joint on this cavity.

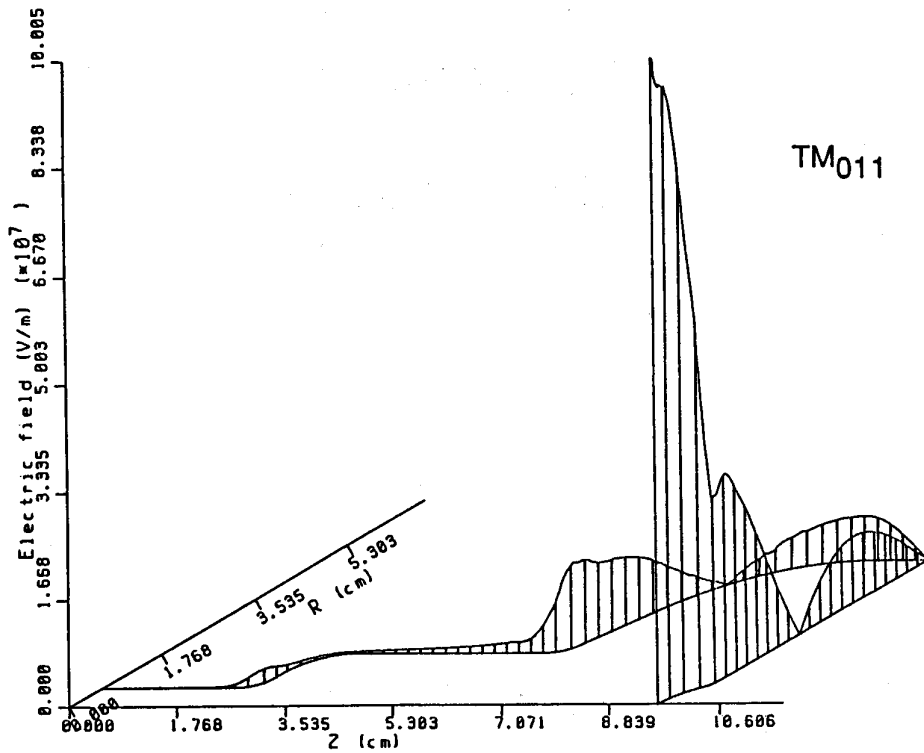


FIGURE 12 Surface electric field of the TM₀₁₁ mode in the Mark II cavity

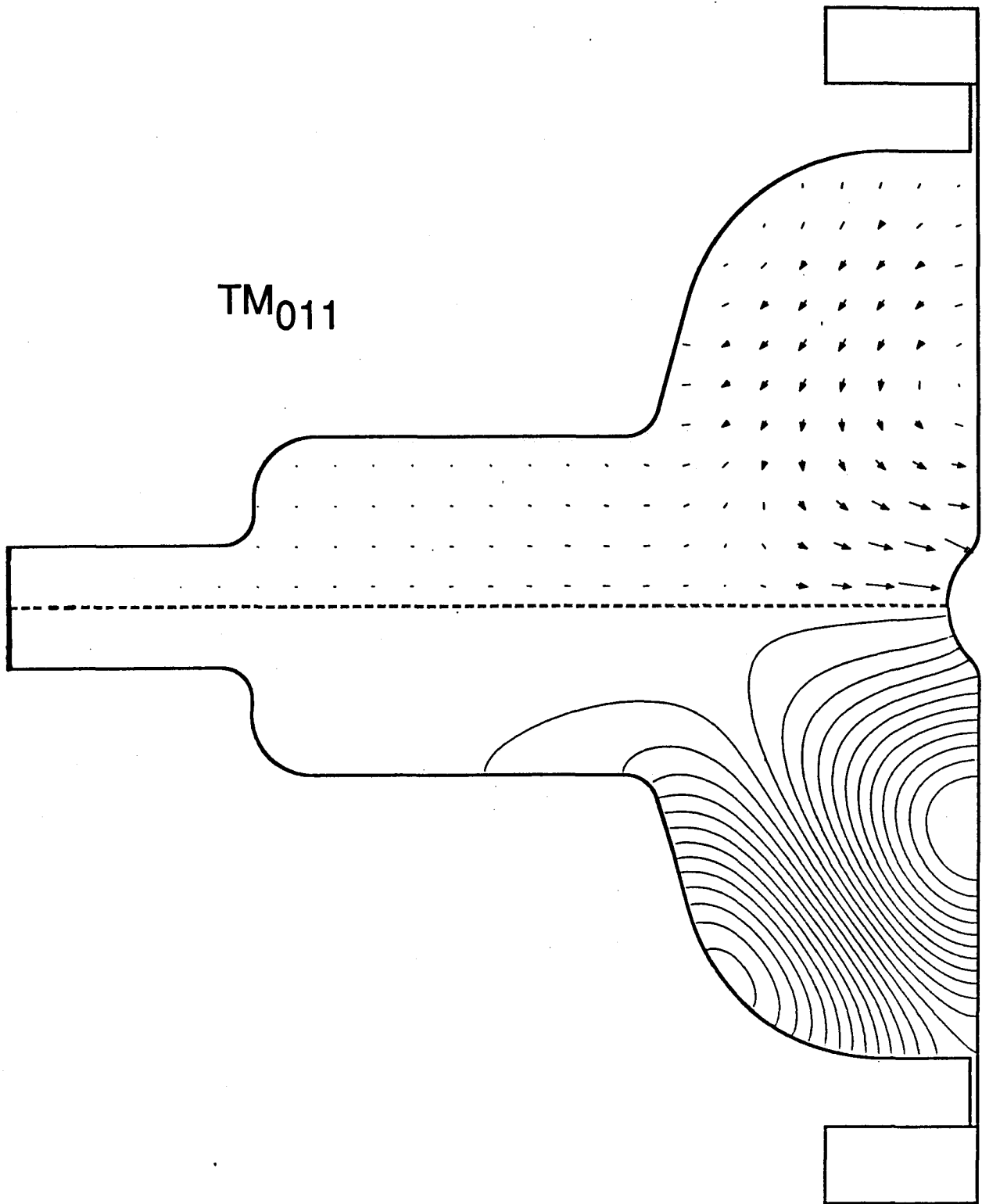


FIGURE 13 Electric field pattern of the TM_{011} mode in the Mark II cavity

field at the cavity corner and the height of the narrow gap joining the groove and cavity. Ideally the field at the corner of the cavity is zero, so the actual cavity design was a poor choice for modelling the behavior of the choke joint. To design the choke joint a coaxial cavity with the same OD as the Mark II cavity was used as the host. The length of the coaxial cavity was such that the frequency of the fundamental mode was the same as the TM_{011} mode in the Mark II cavity. In this mode, the magnetic field is at a maximum at the corners of the coaxial cavity. Using URMEL extensively, the choke joint was tuned to give a current null at the position of the indium joint without perturbing the resonant frequency of the host cavity. A copper model verified the calculations. This joint design was then added to the rest of the Mark II cavity.

The surface electric field for the TM_{011} mode is plotted in Figure 12. The electric field pattern of this mode is shown in Figure 13. It should be noted that in addition to the magnetic field null in the cavity corner, there is also a null in the electric field at the corner of the cavity. The important results from URMEL calculations for the monopole modes of the Mark II cavity are given in Table 4.

TABLE 4

Mark II Monopole Modes

<u>Mode</u>	URMEL calculations			
	<u>MHz</u>	<u>Q_{Cu}</u>	<u>E_{pk}/√U</u>	<u>H_{pk}/E_{pk}</u>
TM ₀₁₀	2747.44	13986	136.0	8.72
TM ₀₂₀	5620.41	16906	121.1	15.1
TM ₀₁₁	6186.81	17598	248.6	10.4
Tube	6931.14			

MV/m/√J G/MV/m

The complete mode spectrum for the Mark II cavity is given in Table 5. These results were also calculated using URMEL. It should also be noted that the input data used for these calculations included the choke joint.

TABLE 5

Mark II Mode Spectrum

<u>Mode type</u>	<u>MHz</u>	<u>Q_{Cu}</u>	<u>G (Ω)</u>	<u>Q_{4.2}</u>	<u>Q_{1.5}</u>
Monopole	1252.28	2679			
Dipole	1618.84	1446			
Quadrupole	2333.29	1139			
TM ₀₁₀	2747.44	13986	191.3	6.27x10 ⁷	5.41x10 ¹⁰
Sextupole	3169.49	1139			
Dipole	3934.37	15691	256.9	4.54	4.04
Dipole	4781.03	18029	325.4	4.13	3.74
Quadrupole	5275.75	17380	329.5	3.55	3.24
TM ₀₂₀	5620.41	16906	330.8	3.20	2.95
Dipole	5781.98	16937	336.1	3.10	2.87
Quadrupole	6082.30	21097	429.4	3.65	3.39
TM ₀₁₁	6186.81	17598	361.3	2.98	2.77
Sextupole	6449.55	18014	377.6	2.91	2.72
Dipole	6542.98	16292	344.0	2.59	2.42
Tube	6931.14	17390	377.9	2.58	2.44

Niobium Cavity Tests

The cavity was first tested with a flat baseplate which was 1/8" in thickness in order to minimize any deflection of the baseplate due to evacuation. This ensured that the frequency of the TM₀₁₁ mode did not stray from the frequency at which the choke joint was designed for maximum effectiveness. The Q₀ at 4.2K was ~3x10⁷ (in agreement with the BCS Q) and the frequency of the TM₀₁₁ mode was 6294 MHz, 108 MHz above the design frequency. The Q₀ at 1.5K at low power was 6.4x10⁹. This is one of the highest Q₀'s ever achieved in a cavity with an indium joint integral to the cavity. Upon raising the power, multipacting immediately followed by thermal breakdown occurred at a peak surface electric field of only 6 MV/m. This barrier could not be processed by either RF or He processing.

Two other modes had Q_0 values in excess of 10^9 . The TM_{020} mode exhibited multipacting and breakdown, but at a field of ~ 6 MV/m. The Q of the beam tube mode was 1.6×10^8 . It is interesting to note that three of the four measurable modes were monopoles. This would imply that the choke joint selectively damped the higher order modes.

A dimpled baseplate was tested next. This plate was 1/16" thick to allow for the drawing of the dimple. To prevent its deflection upon evacuation a brace was welded onto the back. At low power the Q_0 was 8.8×10^9 at 1.5K. The peak surface electric field at this power level was 7.9 MV/m. Unfortunately, upon raising the power 1 dB multipacting and thermal breakdown occurred. In an attempt to process through this barrier the input coupler was inserted quite far into the cavity with the intent of achieving unity coupling in the breakdown state. The power was then raised and processing was observed. The coupler was then backed out and a field of 18 MV/m was attained, but the low power Q_0 had dropped to $\sim 3 \times 10^9$. This sequence was repeated until no further processing was observed. The ultimate field reached was 29 MV/m and was limited by multipacting-induced breakdown.

The source of the multipacting barriers is now under investigation. It has been shown that the choke joint itself is not responsible. The corner of the cavity at the opening of the choke joint, however, appears to be a likely candidate for two-point multipacting.

Summary

Using a specially designed cavity we have been able to establish a record surface RF electric field for niobium of 145 MV/m. The corresponding surface RF magnetic field was 1345 gauss. The test in which these records were established did not indicate what the upper limits to the performance of niobium were, leaving this question unanswered.

Testing of the Mark II cavity is well underway. We have shown that it is possible to achieve Q_0 's in the high 10^9 's with an indium joint. The cavity suffers from heavy multipacting, the source of which has not yet been identified. Once this problem is eliminated emphasis will be placed on understanding the nature of RF field emission and emitters.

References

- [1] Niedermann, P., Experiments on Enhanced Field Emission, PhD Thesis, University of Geneva, 1986

- [2] Citron, A., Compilation of Experimental Results and Operating Experience, Proceedings of the Workshop on RF Superconductivity, Karlsruhe, FRG, 1980, pg. 3-26

- [3] Shu, Q.S., Gendreau, K., Hartung, W., Kirchgessner, J., Moffat, D., Noer, R., Padamsee, H., Rubin, D., Sears, J., R&D in Progress to Overcome Field Emission in Superconducting Accelerator Cavities, Proceedings of the 1989 Particle Accelerator Conference, Chicago, IL

- [4] Amato, J., private communication

- [5] URMEL and URMELT were written by U. Laustroer, U. van Rienen, and T. Weiland, DESY

- [6] SUPERFISH is maintained by the Los Alamos Computer Code Group

- [7] Halbritter, J., Comparison Between Measured and Calculated RF Losses in the Superconducting State, Z. Physik, 238, pg. 466, 1970